Translation of a sphere towards a rigid plane in an Oldroyd-B fluid

Tachin Ruangkriengsin,[1] Rodolfo Brandão,[2] Bimalendu Mahapatra,[3] Evgeniy Boyko,[3] and Howard A. Stone[2,*]

[1]*Program in Applied and Computational Mathematics, Princeton University, Princeton, New Jersey 08544, USA*

[2]*Department of Mechanical and Aerospace Engineering, Princeton University, Princeton, New Jersey 08544, USA*

[3]*Faculty of Mechanical Engineering, Technion – Israel Institute of Technology, Haifa 3200003, Israel*

(Received 10 April 2024; accepted 19 July 2024; published 21 August 2024)

We analyze the low-Reynolds-number translation of a sphere towards or away from a rigid plane in an Oldroyd-B fluid under two scenarios: prescribing the sphere's translational velocity, and prescribing the force on the sphere. Leveraging the lubrication approximation and a perturbation expansion in powers of the Deborah number, we develop a comprehensive theoretical analysis that yields analytical approximations for velocity fields, pressures, and forces acting on the sphere. Our framework aids in understanding temporal microstructural changes as the particle-wall gap evolves over time. In particular, we show that alterations in the polymer conformation tensor in response to geometric changes induce additional forces on the sphere. For cases with prescribed velocity, we present a theoretical approach for calculating resistive forces at any order in the Deborah number and utilize a reciprocal theorem to obtain higher-order corrections based on velocity fields in the previous orders. When the sphere translates with a constant velocity, the fluid viscoelasticity decreases the resistive force at the first order. However, at the second-order correction, the direction of the sphere's movement determines whether viscoelasticity increases or decreases the resistive force. For cases with prescribed force, we show that understanding the influence of viscoelasticity on the sphere's translational velocity necessitates a more intricate analysis even at low Deborah numbers. Specifically, we introduce an ansatz for constant force scenarios, and we derive solution forms for general prescribed forces using the method of multiple scales. We find that when a sphere undergoes sedimentation due to its own weight, the fluid viscoelasticity results in a slower settling process, reducing the leading-order sedimentation rate.

DOI: 10.1103/PhysRevFluids.9.083303

I. INTRODUCTION

The sedimentation of suspensions of particles represents a fundamental aspect of fluid mechanics, influencing processes across numerous fields [1], from blood diagnostics to mineral separations. In Newtonian fluids, the settling behavior of particles follows classical hydrodynamic principles, where gravity, fluid viscosity, and volume fraction dictate the dynamics. However, when dealing with suspensions in non-Newtonian fluids, the situation becomes considerably more complex. Viscoelastic fluids exhibit a range of behaviors, including shear thinning, normal stress differences, and time-dependent responses, which can significantly alter the settling dynamics of suspended particles.

*Contact author: hastone@princeton.edu

For example, in industries such as polymer processing, where viscoelastic fluids are commonplace, controlling particle sedimentation can directly impact product quality and manufacturing efficiency [2,3]. Similarly, in biological systems, the sedimentation of cells and micro-organisms in viscoelastic fluids such as mucus or blood plasma plays a vital role in physiology, affecting health and disease outcomes [4,5]. In this study, our attention is directed toward examining the particle-wall interaction within viscoelastic fluids, employing a simplified sphere model to represent the particle. Our particular emphasis lies on scenarios in which the sphere is in close proximity to the wall, akin to the final stages of its approach towards or away from the surface. Particular attention is given to the time-varying microstructural changes as the particle-wall gap changes in time.

The problem of a sphere translating perpendicular to a plane in Newtonian fluids has been examined comprehensively in recent decades [6–11]. In numerous works, the methodologies employed to address this problem can be extended reciprocally to analyze binary interactions between two spheres moving along the line connecting their centers. The early studies have used bipolar coordinates and derived analytical expressions for the flow field and force on a sphere, which remain valid across arbitrary sphere separations [6–8]. Although these studies have provided a thorough analytical description of a sphere's motion, the majority of findings are presented as infinite series. Other studies focus on situations in which the sphere-wall or sphere-sphere separation is small, enabling the use of asymptotic approximations that are more straightforward to interpret. These approaches include the use of matched asymptotic expansions [9,10] and the lubrication approximation [11].

In comparison to the extensively studied scenarios in Newtonian fluids, there are a limited number of analytical investigations addressing the problem of a sphere translating perpendicular to a plane in non-Newtonian fluids [12–18]. Each study on this topic focuses on a distinct constitutive model and separation distances. Incorporating non-Newtonian effects into the problem poses challenges due to the more complex fluid responses and constitutive descriptions. For instance, experimental exploration of the interaction between two spheres descending along their centerline in a viscoelastic fluid suggests that when the initial separation is small, the spheres eventually approach contact; conversely, when the initial separation is large, they eventually diverge [19].

A commonly utilized model providing an analytical framework for viscoelastic fluid flow problems is the second-order fluid [12–15]. For example, Brunn applied this model to investigate the interaction between two identical sedimenting spheres with a significant initial separation distance, observing a decrease in the distance between spheres as they descended [12]. Subsequently, Ardekani and co-workers studied the motion of a sphere normal to a wall in a second-order fluid under specific classes of normal stress difference, and they conducted an additional analysis using the lubrication approximation [13–15]. Also, other simplified constitutive models have been employed to elucidate the non-Newtonian effects of this problem. In particular, the squeeze flow of a film between two spheres in both power-law [16] and biviscous fluid models has been investigated [17,18], providing essential insights into suspension rheology, especially for fluids exhibiting shear-thinning and shear-thickening behaviors. In this study, we utilize the Oldroyd-B constitutive equation, which is a widely used model in the characterization of constant shear-viscosity Boger fluids [20,21].

Specifically, we investigate scenarios in which the distance between the sphere and the wall is small, allowing us to approximate the flow using the lubrication theory. This approximation has been used widely to analyze particle motion near boundaries in Newtonian fluids, including motions of disks, cylinders, or spheres perpendicular to the wall [22]. Notably, this approximation yields analytical results beyond conventional uniform geometries, extending to scenarios such as sedimentation of particles with zero local curvature or motion of closely fitting particles in tubes [23,24].

In addition to the application of the lubrication approximation to the particle behavior near boundaries in non-Newtonian fluids [13–15], this method, in conjunction with the low Deborah (or Weissenberg) number asymptotic expansion, has been utilized to study pressure-driven flows in narrow nonuniform geometries [25–27], thin-film flows [28–30], and tribology problems [31–33].

Despite advances over the past decades in techniques for obtaining analytical expressions for viscoelastic flows, most studies remain limited to either intrinsically one-dimensional or, in a few cases, two-dimensional flows. Of particular relevance to our work is the squeeze flow of viscoelastic fluids, which is an intrinsically two-dimensional flow, for which exact similarity solutions have been developed for the case of squeeze flow between two parallel plates [34,35]. However, it is important to note that the Oldroyd-B model may not be the most suitable for comparison with experimental results, as it fails to predict the initial stress overshoot observed in experiments [36,37]. Despite this limitation, the analysis using the Oldroyd-B model remains insightful. It provides analytically tractable solutions, which can serve as a foundation for addressing more complex constitutive equations, such as the MPTT model, which accurately represents the experimental data for the squeeze flow [36].

While our work has features similar to the previous studies by Ardekani *et al.* [13] and Dandekar and Ardekani [15], we highlight several distinctions. First, we employ the Oldroyd-B model to characterize viscoelastic fluids, in contrast to the second-order fluid model, which only provides the leading-order effect of viscoelasticity at low Deborah numbers. Thus, using the Oldroyd-B model allows us to obtain higher-order corrections to the force. Furthermore, the Oldroyd-B model offers the advantage of separately understanding polymer stretching dynamics from flow dynamics. In particular, it is important to note that in the case of the squeeze flow configuration, the geometry is time-dependent: it evolves as the sphere translates normal to the wall. This temporal evolution of the geometry leads to temporal changes in polymer stretching, resulting in non-negligible additional polymer stresses. Secondly, unlike the studies of Ardekani *et al.* [13] and Dandekar and Ardekani [15] in which the aspect ratio ϵ, defined in (5), was treated as time-dependent, we maintain a constant aspect ratio and introduce a time-dependent geometry. This allows us to systematically analyze how the changes in the geometry induce the changes in the conformation tensor, and it provides a framework for obtaining higher-order correction solutions. Thirdly, and more importantly, we extend our analysis to scenarios in which the translational velocity is not constant, which provides a more comprehensive understanding of sphere motion. Lastly, we extend our analysis to cases in which the force on the sphere is prescribed, rather than solely focusing on velocity. We show that elucidating the influence of the fluid viscoelasticity on the sphere's dynamics in this force-controlled case requires a more intricate analysis. This scenario is particularly relevant in practical situations, such as when a sphere sediments under its own weight. To the best of our knowledge, this problem remains poorly understood in the context of viscoelastic fluids.

The subsequent sections of this paper are organized as follows: In Sec. II, we formulate the problem and introduce nondimensionalization in line with the lubrication approximation. We also introduce the low-Deborah-number expansion technique, which serves as a foundational tool for our theoretical analysis. In Sec. III, we consider the scenario in which the translational velocity of the sphere is prescribed. We derive the leading-order and first-order correction solutions and then use the reciprocal theorem to obtain the second-order correction. In Sec. IV, we explore the case in which the force on the sphere is prescribed. We consider the case in which the force is constant, and we employ the method of multiple timescales to derive a leading-order long-time asymptotic approximation for more general prescribed force profiles. Finally, we conclude with a discussion of the results in Sec. V.

II. PROBLEM FORMULATION

We examine the translation with velocity $\mathbf{v}(t) = v(t)\mathbf{e}_z$ of a sphere of radius a in a viscoelastic dilute polymer solution towards or away from a rigid planar boundary. Employing cylindrical coordinates (r, θ, z), we consider the time-dependent gap, denoted as $h(r, t)$, between the rigid plane and the sphere, where $h_0(t)$ represents the height at the lowest point of the sphere (see Fig. 1). By this definition, we require that $v(t) = \frac{\mathrm{d}h_0(t)}{\mathrm{d}t}$. In addition, we assume that the initial separation distance $h_0(0)$ between the sphere and the rigid plane satisfies $h_0(0) \ll a$. This condition mirrors the final stage of the approach of an object towards a surface, particularly during the sedimentation process.

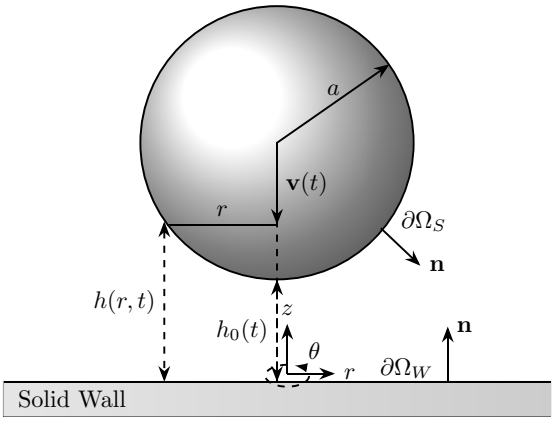

FIG. 1. Schematic illustration of a sphere with radius a translating in a viscoelastic dilute polymer solution and towards a rigid plane.

We employ the Oldroyd-B constitutive model [20,21] to characterize the viscoelastic fluid dynamics within the gap between the sphere and the rigid plane. To provide physical insight into the interplay between the fluid dynamics and the evolution of microstructure in the fluid, which enhances our understanding of their mutual influence, we note that one derivation of the Oldroyd-B constitutive equation involves representing the polymer as a dumbbell structure composed of two particles linked by a linear elastic spring. The fluid flow advects and/or elongates/compresses the polymer, introducing additional stresses and complexity to the fluid behavior. Indeed, as we calculate below, these effects are coupled to the time-varying gap.

An important quantity for understanding the impact of a polymer, or other microstructural element, on the stress tensor is the conformation tensor $\mathbf{A}(r, z, t)$, which characterizes the deformation state of the microstructure. For instance, $\mathbf{A} = \mathbf{I}$ signifies an undistorted equilibrium state of the polymer. As the polymer is suspended within the fluid, it undergoes stretching and advection, leading, in the Oldroyd-B description, to the evolution of the conformation tensor according to

$$\frac{\partial \mathbf{A}}{\partial t} + \mathbf{u} \cdot \nabla \mathbf{A} - \mathbf{A} \cdot \nabla \mathbf{u} - (\nabla \mathbf{u})^T \cdot \mathbf{A} = -\frac{1}{\lambda}(\mathbf{A} - \mathbf{I}), \tag{1}$$

where $\mathbf{u}(r, z, t) = (u_r, 0, u_z)$ is the velocity vector, and λ is the relaxation time of the fluid. When the polymer undergoes stretching away from equilibrium, incremental polymeric stress arises due to the tension in the spring. Consequently, the total stress tensor $\boldsymbol{\sigma}$ for the Oldroyd-B model can be expressed as

$$\boldsymbol{\sigma} = -p\mathbf{I} + 2\mu_s \mathbf{E} + \frac{\mu_p}{\lambda}(\mathbf{A} - \mathbf{I}). \tag{2}$$

In Eq. (2), the first term denotes the pressure component and the second term denotes the viscous stress from the solvent with viscosity μ_s, where $\mathbf{E} = \frac{1}{2}[\nabla \mathbf{u} + (\nabla \mathbf{u})^T]$ is the rate-of-strain tensor. The last term denotes the polymeric contribution to the stress, where μ_p corresponds to the polymer viscosity at zero shear rate, and μ_p/λ represents the elastic modulus of the fluid.

Finally, we consider the low-Reynolds-number limit of the flow as we assume that the effective Reynolds number is small under the assumption that $h_0(0) \ll a$, which allows us to neglect inertial effects. In this scenario, the fluid motion is governed by the continuity and momentum equations,

$$\nabla \cdot \mathbf{u} = 0 \quad \text{and} \quad \nabla \cdot \boldsymbol{\sigma} = \mathbf{0}. \tag{3}$$

Equations (1), (2), and (3) form the basis of the Oldroyd-B model for the axisymmetric flow problem we investigate in this work. These equations are coupled with the no-slip and no-penetration boundary conditions along the surface of the sphere and the rigid plane:

$$u_r = 0 \quad \text{at} \quad z = 0, \quad u_r = 0 \quad \text{at} \quad z = h(r,t), \tag{4a}$$

$$u_z = 0 \quad \text{at} \quad z = 0, \quad u_z = v(t) \quad \text{at} \quad z = h(r,t). \tag{4b}$$

A. Nondimensionalization

The motion of the sphere is governed by the flow in the confined space between the particle surface and the rigid plane, which we describe using a lubrication theory. In this limit, the flow outside the gap makes a subdominant contribution to the hydrodynamic force on the sphere. In the local context where $h_0 \ll a$, the gap geometry exhibits a parabolic variation with r, described by $h \approx h_0(1 + \frac{r^2}{2ah_0})$. Thus, we choose the characteristic lengthscale along the gap in the r-direction as $\sqrt{2ah_0(0)}$ and the characteristic lengthscale along the z-direction as $h_0(0)$. Therefore, the aspect ratio ϵ of the configuration is

$$\epsilon = \frac{h_0(0)}{\sqrt{2ah_0(0)}} = \sqrt{\frac{h_0(0)}{2a}} \ll 1. \tag{5}$$

With these lengthscales, and choosing the initial speed $|v(0)|$ as the characteristic velocity, we introduce nondimensional variables based on the lubrication approximation,

$$\begin{aligned} Z &= \frac{z}{h_0(0)}, \quad R = \frac{r}{\sqrt{2ah_0(0)}}, \quad H = \frac{h}{h_0(0)} = H_0(T) + R^2, \\ H_0 &= \frac{h_0(t)}{h_0(0)}, \quad V = \frac{v(t)}{|v(0)|}, \quad U_R = \frac{h_0(0)u_r}{|v(0)|\sqrt{2ah_0(0)}}, \quad U_Z = \frac{u_z}{|v(0)|}, \\ \boldsymbol{\mathcal{E}} &= \frac{h_0(0)^2\mathbf{E}}{|v(0)|\sqrt{2ah_0(0)}}, \quad P = \frac{h_0(0)^2 p}{2\mu|v(0)|a}, \quad F = \frac{h_0(0)f}{4\mu|v(0)|a^2}. \end{aligned} \tag{6}$$

Here, $\mu = \mu_s + \mu_p$ is the total zero-shear-rate viscosity of the polymer solution, and f is the resistive force acting on the sphere. Also, given the unsteady nature of the problem, we define the timescale $T = \frac{|v(0)|t}{h_0(0)}$ based on a typical flow timescale for the sphere's translation. In addition, by considering a balance between the Newtonian viscous stress and the polymer shear stress, along with the assumption that the conformation tensor remains finite as $\epsilon \to 0$, and then using length and velocity scales in (6), we set [26,28,29,31,32]

$$\mathcal{A}_{RR} = \epsilon^2 A_{rr} = \frac{h_0(0)A_{rr}}{2a}, \quad \mathcal{A}_{RZ} = \epsilon A_{rz} = \frac{h_0(0)A_{rz}}{\sqrt{2ah_0(0)}}, \quad \mathcal{A}_{ZZ} = A_{zz}, \tag{7}$$

where A_{ij} are the components of the conformation tensor $\mathbf{A}$. These dimensionless variables are supplemented with additional dimensionless parameters for viscosity ratios,

$$\beta_p = \frac{\mu_p}{\mu} = \frac{\mu_p}{\mu_s + \mu_p} \quad \text{and} \quad \beta_s = 1 - \beta_p, \tag{8}$$

and the Deborah number

$$\mathrm{De} = \frac{\lambda|v(0)|}{h_0(0)}. \tag{9}$$

The Deborah number De characterizes the ratio of the characteristic time for the material to respond to deformation, λ, to the characteristic time of the flow process, $h_0(0)/|v(0)|$. As is well known, De measures the degree of material viscoelasticity and helps identify whether the material exhibits elastic or viscous behavior under given flow conditions. It should be noted that we define the Deborah number based on the initial velocity and height of the sphere. In general, both the velocity

and height may change significantly during motion, thereby altering the viscoelastic effects. Despite this, we proceed with our analysis under the assumption that the order of magnitude for both the velocity (v) and the height (h_0) do not vary substantially as the sphere translates towards the rigid plane.

B. Governing equations in dimensionless form

By substituting the nondimensional variables introduced in (6)–(9) and neglecting $O(\epsilon^2)$ terms, consistent with the lubrication approximation, the governing equations (1)–(3) for the axisymmetric sphere-translation problem in cylindrical coordinates are expressed as

$$0 = \frac{1}{R}\frac{\partial(RU_R)}{\partial R} + \frac{\partial U_Z}{\partial Z}, \tag{10a}$$

$$0 = -\frac{\partial P}{\partial R} + \beta_s \frac{\partial^2 U_R}{\partial Z^2} + \frac{\beta_p}{\mathrm{De}}\left(\frac{1}{R}\frac{\partial(R\mathcal{A}_{RR})}{\partial R} + \frac{\partial \mathcal{A}_{RZ}}{\partial Z}\right), \tag{10b}$$

$$0 = \frac{\partial P}{\partial Z}, \tag{10c}$$

$$-\frac{1}{\mathrm{De}}\mathcal{A}_{RR} = \frac{\partial \mathcal{A}_{RR}}{\partial T} + U_R\frac{\partial \mathcal{A}_{RR}}{\partial R} + U_Z\frac{\partial \mathcal{A}_{RR}}{\partial Z} - 2\mathcal{A}_{RR}\frac{\partial U_R}{\partial R} - 2\mathcal{A}_{RZ}\frac{\partial U_R}{\partial Z}, \tag{10d}$$

$$-\frac{1}{\mathrm{De}}\mathcal{A}_{RZ} = \frac{\partial \mathcal{A}_{RZ}}{\partial T} + U_R\frac{\partial \mathcal{A}_{RZ}}{\partial R} + U_Z\frac{\partial \mathcal{A}_{RZ}}{\partial Z} - \mathcal{A}_{RR}\frac{\partial U_Z}{\partial R} - \mathcal{A}_{ZZ}\frac{\partial U_R}{\partial Z} - \mathcal{A}_{RZ}\left(\frac{\partial U_Z}{\partial Z} + \frac{\partial U_R}{\partial R}\right), \tag{10e}$$

$$-\frac{1}{\mathrm{De}}(\mathcal{A}_{ZZ} - 1) = \frac{\partial \mathcal{A}_{ZZ}}{\partial T} + U_R\frac{\partial \mathcal{A}_{ZZ}}{\partial R} + U_Z\frac{\partial \mathcal{A}_{ZZ}}{\partial Z} - 2\mathcal{A}_{ZZ}\frac{\partial U_Z}{\partial Z} - 2\mathcal{A}_{RZ}\frac{\partial U_Z}{\partial R}. \tag{10f}$$

It is important to highlight that from the momentum equation in the z-direction, Eq. (10c), it follows that the pressure only varies in the r-direction, i.e., $P = P(R, T)$. Even though the problem is axisymmetric, the components of the conformation tensor $\mathbf{A}$ in the θ-direction ($\mathcal{A}_{\theta R}$, $\mathcal{A}_{\theta Z}$, $\mathcal{A}_{\theta\theta}$) are, however, not constants and evolve as per Eq. (1). These terms do not influence the momentum balance and the evolution of $\mathbf{A}$ in the r- and z-directions due to the lubrication approximation, and so they are not presented.

Employing nondimensional variables, the corresponding boundary conditions (4) can be expressed as

$$U_R = 0 \quad \text{at} \quad Z = 0, \quad U_R = 0 \quad \text{at} \quad Z = H(R, T), \tag{11a}$$

$$U_Z = 0 \quad \text{at} \quad Z = 0, \quad U_Z = V(T) \quad \text{at} \quad Z = H(R, T), \tag{11b}$$

with $H_0(0) = 1$ and $V(0) = \mathrm{sgn}(v(0))$.

Observe that the momentum equation (10b) relies solely on U_R and not U_Z. Thus, it is convenient to reformulate the continuity equation (10a) to a form that exclusively involves the term U_R. To this end, we proceed with our calculation akin to the derivation of the Reynolds equation of classical lubrication theory [38]. We integrate both sides of the continuity equation (10a) with respect to Z from 0 to H and utilize the boundary conditions to obtain

$$\begin{aligned} 0 &= \int_0^H \left(\frac{1}{R}\frac{\partial(RU_R)}{\partial R} + \frac{\partial U_Z}{\partial Z}\right)\mathrm{d}Z = \int_0^H \left(\frac{1}{R}\frac{\partial(RU_R)}{\partial R}\right)\mathrm{d}Z + V(T) \\ &= \frac{1}{R}\frac{\partial}{\partial R}\left(R\int_0^H U_R\,\mathrm{d}Z\right) + V(T). \end{aligned} \tag{12}$$

Note that the second and third equalities are derived from the boundary conditions (11). Subsequently, we integrate both sides of Eq. (12) with respect to R and assume that the velocity remains

bounded at $R = 0$, resulting in

$$\int_0^H U_R \, \mathrm{d}Z = -\frac{RV(T)}{2}. \tag{13}$$

This form of the continuity equation will be employed for calculations throughout this paper.

C. Low-Deborah-number expansion

In the following sections, we consider the weakly viscoelastic limit $\mathrm{De} \ll 1$. Our approach relies on regular perturbation expansions, ordered by the Deborah number, for the unknown variables such as velocity, pressure, and components of the conformation tensor. In scenarios in which we impose a force on the sphere, we also extend this perturbation analysis to the height and velocity of the sphere. We express any unknown quantity $\mathcal{S}$ as

$$\mathcal{S} = \mathcal{S}^{(0)} + \mathrm{De}\mathcal{S}^{(1)} + \mathrm{De}^2\mathcal{S}^{(2)} + \cdots, \tag{14}$$

where the superscript indicates the corresponding order in De.

Before we proceed further, we utilize the evolution equations for the components of the conformation tensor (10d)–(10f) to write the corresponding expansion at a given order in terms of velocity fields of lower orders. This proceeds order-by-order as follows:

(1) As an initial condition, we assume that before the sphere starts to translate, the viscoelastic fluid is fully relaxed, $\mathbf{A} = \mathbf{I}$. In the lubrication limit and $\mathrm{De} \to 0$, the evolution equations for the conformation tensor components (10d)–(10f) yield

$$\mathcal{A}_{ZZ}^{(0)} = 1, \quad \mathcal{A}_{RZ}^{(0)} = 0, \quad \mathcal{A}_{RR}^{(0)} = 0. \tag{15}$$

(2) Using (15), we express the conformation tensor components at the first order, $O(\mathrm{De})$, as

$$\mathcal{A}_{ZZ}^{(1)} = 2\frac{\partial U_Z^{(0)}}{\partial Z}, \quad \mathcal{A}_{RZ}^{(1)} = \frac{\partial U_R^{(0)}}{\partial Z}, \quad \mathcal{A}_{RR}^{(1)} = 0. \tag{16}$$

At this order, the temporal changes in $\boldsymbol{\mathcal{A}}^{(1)}$ are incorporated through the temporal changes in the leading-order velocity field; the changes in the conformation tensor $\frac{\partial \boldsymbol{\mathcal{A}}^{(0)}}{\partial T}$ do not contribute to the values of $\boldsymbol{\mathcal{A}}^{(1)}$.

(3) At second order, $O(\mathrm{De}^2)$ and beyond, the conformation tensor components are influenced by the time derivative $\frac{\partial \mathbf{A}}{\partial T}$ at a lower order. This dependency arises due to the temporal evolution of the velocity fields, as the geometry changes in time. For example, at the second order, $O(\mathrm{De}^2)$, we have

$$\mathcal{A}_{ZZ}^{(2)} = -2\frac{\partial^2 U_Z^{(0)}}{\partial T \partial Z} - 2U_R^{(0)}\frac{\partial^2 U_Z^{(0)}}{\partial R \partial Z} - 2U_Z^{(0)}\frac{\partial^2 U_Z^{(0)}}{\partial Z^2} + 2\frac{\partial U_Z^{(1)}}{\partial Z} + 4\left(\frac{\partial U_Z^{(0)}}{\partial Z}\right)^2 + 2\frac{\partial U_Z^{(0)}}{\partial R}\frac{\partial U_R^{(0)}}{\partial Z}, \tag{17a}$$

$$\mathcal{A}_{RZ}^{(2)} = -\frac{\partial^2 U_R^{(0)}}{\partial T \partial Z} - U_R^{(0)}\frac{\partial^2 U_R^{(0)}}{\partial R \partial Z} - U_Z^{(0)}\frac{\partial^2 U_R^{(0)}}{\partial Z^2} + 2\frac{\partial U_Z^{(0)}}{\partial Z}\frac{\partial U_R^{(0)}}{\partial Z} + \frac{\partial U_R^{(1)}}{\partial Z} - \frac{U_R^{(0)}}{R}\frac{\partial U_R^{(0)}}{\partial Z}, \tag{17b}$$

$$\mathcal{A}_{RR}^{(2)} = 2\left(\frac{\partial U_R^{(0)}}{\partial Z}\right)^2. \tag{17c}$$

Despite neglecting inertial effects in the momentum equation (10b), time derivatives of the velocity field influence the conformation tensor components, specifically through $\frac{\partial \mathbf{A}}{\partial T}$.

In the next sections, we explore two distinct scenarios. First, we examine the situation in which we prescribe the translational velocity of the sphere. In this case, our focus is on understanding the pressure and forces experienced by the sphere. Second, we investigate the case in which an applied force is prescribed to the sphere. Here, our interest lies in understanding the velocity of the

sphere. Notably, the first case yields a more straightforward solution structure, offering clarity on the fundamental steps and concepts in our calculations. On the other hand, the second case, although more challenging to solve, aligns more closely with physical scenarios, such as the sedimentation of the sphere under its own weight or the motion of a spherical tip of an atomic force microscope towards or away from a substrate surrounded by a viscoelastic fluid.

III. TRANSLATION OF A SPHERE UNDER A PRESCRIBED VELOCITY

In this section, we consider the case in which the sphere's translational velocity $V(T) = \frac{\mathrm{d}H_0}{\mathrm{d}T}$ is known. Our objective is to compute the resistive force exerted on the sphere as it translates through a viscoelastic fluid. To this end, we provide a systematic analysis by solving order by order the hydrodynamic problem.

A. Leading-order solution

When De $\ll 1$, the fluid displays a weakly viscoelastic behavior. Thus, we anticipate the leading-order solution to closely resemble the Newtonian solution, with viscoelastic effects showing up as "corrections" in subsequent orders. To show that, we substitute (16) into (10b) to yield

$$0 = -\frac{\partial P^{(0)}}{\partial R} + \beta_s \frac{\partial^2 U_R^{(0)}}{\partial Z^2} + \beta_p \left(\frac{1}{R} \frac{\partial \left(R \mathcal{A}_{RR}^{(1)} \right)}{\partial R} + \frac{\partial \mathcal{A}_{RZ}^{(1)}}{\partial Z} \right) \tag{18a}$$

$$= -\frac{\partial P^{(0)}}{\partial R} + \beta_s \frac{\partial^2 U_R^{(0)}}{\partial Z^2} + \beta_p \left(\frac{\partial}{\partial Z} \left(\frac{\partial U_R^{(0)}}{\partial Z} \right) \right) = -\frac{\partial P^{(0)}}{\partial R} + \frac{\partial^2 U_R^{(0)}}{\partial Z^2}. \tag{18b}$$

Equation (18b) is the classical low-Reynolds-number momentum equation of a Newtonian fluid with a constant viscosity μ often encountered in lubrication calculations. We integrate (18b) twice with respect to Z and use the boundary conditions (11) to obtain

$$U_R^{(0)} = \frac{1}{2} \frac{\partial P^{(0)}}{\partial R} Z(Z - H). \tag{19}$$

Recall that the velocity of the sphere is known. Therefore, V only occurs in the leading order of the expansion. In particular, the continuity equation in the form we have previously discussed (13) now is written $\int_0^H U_R^{(0)} \, \mathrm{d}Z = -\frac{RV}{2}$. Using this expression together with (19) gives

$$\frac{\partial P^{(0)}}{\partial R} = \frac{6RV}{H^3} \Longrightarrow P^{(0)} = -\frac{3V}{2H^2}, \tag{20}$$

where we assume that the reference pressure in the far field ($R \to \infty$) is zero.

Subsequently, we evaluate the resistive force exerted on the sphere by the viscoelastic fluid. Intuitively, in the lubrication limit, we anticipate that the primary contribution to the resistive force arises from the pressure along the gap rather than from the viscous and polymeric stresses. To show this, we recall that the normal stress near the bottom of the sphere is $\sigma_{zz} = -p + 2\mu_s \frac{\partial u_z}{\partial z} + \frac{\mu_p}{\lambda}(A_{zz} - 1)$. Thus, using the nondimensional variables (6), we arrive at an expression for the nondimensional normal stress,

$$\Sigma_{ZZ} = \frac{h_0(0)^2 \sigma_{zz}}{2\mu |v(0)| a} = -P(R,T) + 2\epsilon^2 \left(\beta_s \frac{\partial U_Z}{\partial Z} + \frac{\beta_p}{2\mathrm{De}} (\mathcal{A}_{ZZ} - 1) \right) = -P(R,T) + O(\epsilon^2). \tag{21}$$

Equation (21) shows that the major contribution to the resistive force acting on the sphere in the lubrication limit is due to the pressure, rather than the viscous force and the polymeric stress. The

leading-order solution for the vertical force acting on the sphere can then be derived by integrating the leading-order stress (21) on the surface $\partial\Omega_S$ of the sphere,

$$F^{(0)} = \mathbf{e}_z \cdot \int_{\partial\Omega_S} \mathbf{n} \cdot \Sigma^{(0)} \, \mathrm{d}S \approx -\int_{\partial\Omega_S} \Sigma^{(0)}_{ZZ} \, \mathrm{d}S = -2\pi \int_0^\infty \frac{3VR}{2H^2} \, \mathrm{d}R = -\frac{3\pi V}{2H_0}, \tag{22}$$

where the integration can be taken to $R \to \infty$ because the relevant length $\sqrt{2ah(0)} \ll a$. Therefore, we have demonstrated that the leading-order solution for the weakly viscoelastic fluid resembles the conventional Newtonian solution [39]. Nevertheless, as we next show, viscoelastic effects arise at the next-order corrections, where the leading-order velocity field creates changes of the conformation tensor.

B. First-order correction

Similar to the steps we have used to obtain the leading-order solution, we proceed with our calculations by solving for the velocity in terms of the pressure gradient through the momentum equation, utilizing the continuity equation to solve for pressure, and ultimately integrating the pressure to determine the resistive force acting on the sphere. First, using the second-order correction of the components of the conformation tensor we have previously calculated, (17a)–(17c), we simplify the first-order correction for the momentum equation (10b),

$$0 = -\frac{\partial P^{(1)}}{\partial R} + \beta_s \frac{\partial^2 U_R^{(1)}}{\partial Z^2} + \beta_p \left(\frac{1}{R} \frac{\partial \left(R \mathcal{A}^{(2)}_{RR} \right)}{\partial R} + \frac{\partial \mathcal{A}^{(2)}_{RZ}}{\partial Z} \right) \tag{23a}$$

$$= -\frac{\partial P^{(1)}}{\partial R} + \frac{\partial^2 U_R^{(1)}}{\partial Z^2} + \beta_p \left(-\frac{\partial}{\partial T} \left(\frac{6RV}{H^3} \right) - \frac{36RV^2 [R^4 + H_0(R^2 - 2Z) - 2R^2 Z + 2Z^2]}{H^6} \right). \tag{23b}$$

Unlike the leading-order solution, we observe the emergence of conformation tensor components in the first-order correction of the momentum equation. Next, we integrate (23b) twice with respect to Z to obtain an expression for radial velocity in terms of the pressure gradient,

$$U_R^{(1)} = \frac{1}{2} \frac{\partial P^{(1)}}{\partial R} (Z)(Z - H) + \beta_p \left(\frac{\partial}{\partial T} \left(\frac{3RV}{H^3} \right) (Z)(Z - H) + \frac{6RV^2 Z \left[H_0^3 + H_0(-3R^4 + 3R^2 Z - 2Z^2) + Z^3 - 2R^2 Z^2 + 3R^4 Z - 2R^6 \right]}{H^6} \right). \tag{24}$$

Using the continuity equation (13), which at the first order is $\int_0^H U_R^{(1)} \, \mathrm{d}Z = 0$, we obtain the first-order correction to the pressure as

$$P^{(1)} = \beta_p \left(\underbrace{\frac{3}{2H^2} \frac{\mathrm{d}V}{\mathrm{d}T} - \frac{3V^2}{H^3}}_{\text{from } \frac{\partial \mathbf{A}}{\partial T}} - \frac{9V^2 (H_0 - 4R^2)}{10H^4} \right), \tag{25}$$

where we have indicated that the temporal variation in the conformation tensor introduces additional pressure terms, which are non-negligible even when the velocity V is constant. Finally, we integrate the first-order correction of pressure (25) to determine the first-order correction to the resistive force

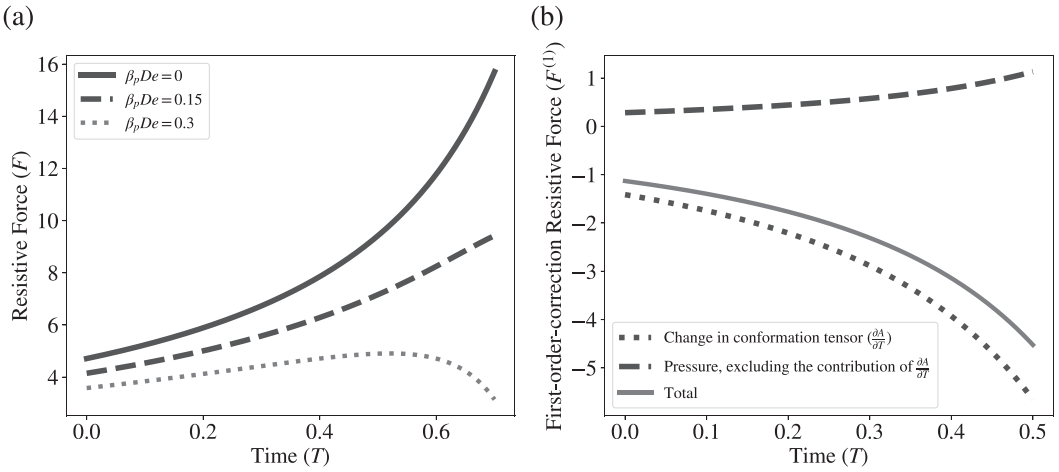

FIG. 2. (a) The time evolution of the resistive force, up to the first-order correction in De, acting on the sphere translating towards the plane with a constant velocity in an Oldroyd-B fluid for different values of β_pDe. (b) Contributions to the first-order correction to the resistive force acting on the sphere translating towards the plane with a constant velocity in an Oldroyd-B fluid with $\beta_p\mathrm{De} = 0.3$.

acting on the sphere:

$$F^{(1)} = 2\pi \int_0^\infty RP^{(1)}\,\mathrm{d}R = \pi\beta_p \left(\underbrace{\frac{3}{2H_0}\frac{\mathrm{d}V}{\mathrm{d}T} - \frac{3V^2}{2H_0^2}}_{\text{from } \frac{\partial \mathbf{A}}{\partial T}} + \frac{3V^2}{10H_0^2} \right) = \pi\beta_p \left(\frac{3}{2H_0}\frac{\mathrm{d}V}{\mathrm{d}T} - \frac{6V^2}{5H_0^2} \right). \tag{26}$$

Note that, for a constant velocity V, our result (26) agrees with the first-order correction to the resistive force obtained using the second-order fluid model by Ardekani *et al.* [13].

In Fig. 2(a), we illustrate the time evolution of the resistive force up to the first-order correction for different values of β_pDe. We observe that the fluid viscoelasticity diminishes the resistive force, and such a reduction becomes more prominent at higher Deborah numbers (De). Figure 2(b) shows the time evolution of the first-order correction to the resistive force and its two contributions. We note that the changes in the conformation tensor (black dotted curve) contribute negatively to the first-order correction, resulting in an overall negative value for this correction.

C. Reciprocal theorem for the next higher-order correction

The procedure outlined in Sec. III B can be applied to derive higher-order corrections for the velocity field, conformation tensor components, pressure, and resistive force. However, as hinted in Sec. III B, the calculations become exceedingly intricate with each successive order. To overcome this challenge, we introduce a calculation strategy, akin to the Lorentz reciprocal theorem, to deduce the next-order correction to the resistive force solely from solutions at the preceding order [25]. This approach circumvents the necessity to calculate velocity fields and pressures in advance. We use this approach to obtain the second-order correction to the resistive force.

To this end, we consider an auxiliary problem of a sphere translating normal to a rigid plane with the same velocity in a Newtonian fluid of viscosity $\mu = \mu_s + \mu_p$,

$$\boldsymbol{\nabla}\cdot\hat{\mathbf{u}} = 0, \quad \boldsymbol{\nabla}\cdot\hat{\boldsymbol{\sigma}} = \mathbf{0}, \quad \text{where} \quad \hat{\boldsymbol{\sigma}} = -\hat{p}\mathbf{I} + 2(\mu_s + \mu_p)\hat{\mathbf{E}}, \tag{27}$$

with the no-slip boundary conditions:

$$\hat{u}_r = 0 \quad \text{at} \quad z = 0, \quad \hat{u}_r = 0 \quad \text{at} \quad z = h(r,t), \tag{28a}$$

$$\hat{u}_z = 0 \quad \text{at} \quad z = 0, \quad \hat{u}_z = v(t) \quad \text{at} \quad z = h(r,t). \tag{28b}$$

We combine (2), (3), and (27), and recall that $\mathbf{A}$ is a symmetric tensor, to obtain

$$\nabla \cdot (\boldsymbol{\sigma} \cdot \hat{\mathbf{u}}) - \nabla \cdot (\hat{\boldsymbol{\sigma}} \cdot \mathbf{u}) = \boldsymbol{\sigma} : \nabla \hat{\mathbf{u}} - \hat{\boldsymbol{\sigma}} : \nabla \mathbf{u} = \frac{\mu_p}{\lambda} \mathbf{A} : \nabla \hat{\mathbf{u}} - 2\mu_p \hat{\mathbf{E}} : \nabla \mathbf{u}$$

$$= \mu_p \left(\frac{1}{\lambda} \mathbf{A} : \hat{\mathbf{E}} - 2\mathbf{E} : \hat{\mathbf{E}} \right). \tag{29}$$

First, we integrate the left-hand side of (29) across the control volume Ω between the sphere and the wall and use the divergence theorem with the boundary conditions (4) and (28) to obtain

$$\int_\Omega (\nabla \cdot (\boldsymbol{\sigma} \cdot \hat{\mathbf{u}}) - \nabla \cdot (\hat{\boldsymbol{\sigma}} \cdot \mathbf{u}))\, \mathrm{d}\Omega = \int_{\partial\Omega_W} (-\mathbf{n} \cdot \boldsymbol{\sigma} \cdot \hat{\mathbf{u}} + \mathbf{n} \cdot \hat{\boldsymbol{\sigma}} \cdot \mathbf{u})\, \mathrm{d}S + \int_{\partial\Omega_S} (-\mathbf{n} \cdot \boldsymbol{\sigma} \cdot \hat{\mathbf{u}} + \mathbf{n} \cdot \hat{\boldsymbol{\sigma}} \cdot \mathbf{u})\, \mathrm{d}S \tag{30a}$$

$$= v \int_{\partial\Omega_S} (-\mathbf{n} \cdot \boldsymbol{\sigma} \cdot \mathbf{e}_z + \mathbf{n} \cdot \hat{\boldsymbol{\sigma}} \cdot \mathbf{e}_z)\, \mathrm{d}S = v(\hat{f} - f), \tag{30b}$$

where $\mathbf{n}$ is the normal directed into the fluid and $\partial\Omega_{W,S}$ are the boundary of the wall and the sphere, respectively; this calculation brings in the hydrodynamic forces f and $\hat{f}$. Second, we seek to simplify the volume integral from (29), $\mu_p \int_\Omega (\frac{1}{\lambda} \mathbf{A} : \hat{\mathbf{E}} - 2\mathbf{E} : \hat{\mathbf{E}})\, \mathrm{d}\Omega$, to equate the result with (30b). Given the lubrication approximation introduced in Sec. II A, and reverting to rescaled variables, we have the rate-of-strain tensor,

$$\boldsymbol{\mathcal{E}} = \frac{1}{2} \left(\frac{\partial U_R}{\partial Z} \right) (\mathbf{e}_r \mathbf{e}_z + \mathbf{e}_z \mathbf{e}_r) + O(\epsilon) \Longrightarrow 2\boldsymbol{\mathcal{E}} : \hat{\boldsymbol{\mathcal{E}}} = \frac{\partial U_R}{\partial Z} \frac{\partial \hat{U}_R}{\partial Z} + O(\epsilon^2). \tag{31}$$

Similarly, we find $\boldsymbol{\mathcal{A}} : \hat{\boldsymbol{\mathcal{E}}} = \mathcal{A}_{RR} \frac{\partial \hat{U}_R}{\partial R} + \mathcal{A}_{RZ} \frac{\partial \hat{U}_R}{\partial Z} + O(\epsilon^2)$. Combining these results together and using the fact that the solution to the auxiliary problem (27) is the same as the leading-order solution for the velocity field we have derived in Sec. III A, we obtain a general formula for calculating the resistive force on the sphere,

$$F = \hat{F} - \frac{\beta_p}{V} \int_\Omega \left(\frac{1}{\mathrm{De}} \left(\mathcal{A}_{RR} \frac{\partial \hat{U}_R}{\partial R} + \mathcal{A}_{RZ} \frac{\partial \hat{U}_R}{\partial Z} \right) - \frac{\partial U_R}{\partial Z} \frac{\partial \hat{U}_R}{\partial Z} \right) \mathrm{d}\Omega + O(\epsilon^2) \tag{32a}$$

$$\approx -\frac{3\pi V}{2H_0} - \frac{2\pi\beta_p}{V} \int_0^\infty \int_0^H R \left(\frac{1}{\mathrm{De}} \left(\mathcal{A}_{RR} \frac{\partial U_R^{(0)}}{\partial R} + \mathcal{A}_{RZ} \frac{\partial U_R^{(0)}}{\partial Z} \right) - \frac{\partial U_R}{\partial Z} \frac{\partial U_R^{(0)}}{\partial Z} \right) \mathrm{d}Z\mathrm{d}R, \tag{32b}$$

where we have assumed that the integrals decay sufficiently fast enough in R so that we may extend the integrals to infinity.

Note that we have verified that the first-order correction to the resistive force obtained through the reciprocal theorem agrees with the calculations from the previous section. In addition, we apply this approach to directly determine the second-order correction to the force, and we find

$$F^{(2)} = \pi\beta_p \left(\frac{(-3150 + 12\beta_p)V^3}{1750H_0^3} + \frac{18V}{5H_0^2} \frac{\mathrm{d}V}{\mathrm{d}T} - \frac{3}{2H_0} \frac{\mathrm{d}^2V}{\mathrm{d}T^2} \right). \tag{33}$$

It is evident from Eq. (33) that for a constant velocity V, the viscoelasticity of the polymer solution can either increase or decrease the resistive force at the second order, depending on the sign of V. Specifically, when the sphere translates towards the wall ($V < 0$), the second-order correction to the resistive forces is positive, and vice versa. We illustrate the effect of this second-order correction in Fig. 3. To ensure that the asymptotic expansion in Deborah number (14) is valid, we require the

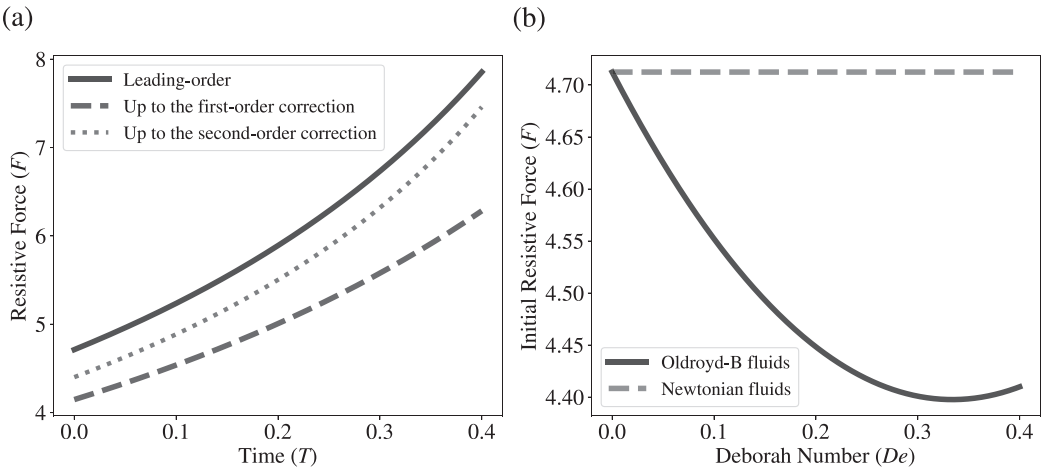

FIG. 3. (a) The time evolution of the resistive force acting on the sphere translating towards a rigid plane with a constant velocity in an Oldroyd-B fluid for De $= 0.3$ and $\beta_p = 0.5$. The solid line represents the leading-order resistive force. The dashed line represents the resistive force up to the first-order correction. The dotted line represents the resistive force up to the second-order correction. (b) Initial resistive force at $T = 0$, up to the second-order correction in De, acting on the sphere translating towards a rigid plane with a constant velocity in an Oldroyd-B fluid as a function of De for $\beta_p = 0.5$. The dashed line represents the behavior of a Newtonian fluid, and the solid line represents the behavior of an Oldroyd-B fluid.

magnitude of the second-order correction term to be smaller than that of the first-order correction term. For instance, considering the resistive force at the initial time $T = 0$, by inspecting (26) and (33), we need De $\lessapprox 2/3$ for the approximation to remain valid; we plot the initial resistive force up to the second-order correction in De for $0 \leqslant$ De $\leqslant 0.4$ in Fig. 3. Nevertheless, when such an assumption holds, the resistive force up to the second-order correction exhibits the same trend as the resistive force up to the first-order correction, where polymer solutions reduce the resistive force from a Newtonian solvent.

The resistive force results we have derived can also be applied to scenarios with nonconstant translational velocity. A particularly useful case is oscillatory movements, where the sphere undergoes periodic motion normal to the rigid plane. This scenario is relevant for rheology measurements, such as using a spherical probe to assess the viscoelasticity of protein condensates [40,41]. In this situation, the sphere oscillates at a distance $h_0(0)$ from the rigid plane with an amplitude γ, described by $h_0 = h_0(0) - \gamma \sin \omega t$. Using the scalings in (6), we obtain the resistive force acting on the sphere (22), (26), and (33), depending on the dimensionless amplitude $\Gamma = \frac{\gamma}{h_0(0)}$, De, and β_p; we plot this result in Fig. 4. Similar to the case with constant velocity, we observe that viscoelasticity reduces the amplitude of the resistive force compared to Newtonian fluids and introduces a phase lag due to the polymer's relaxation time.

IV. TRANSLATION OF A SPHERE UNDER A PRESCRIBED FORCE

In this section, we examine the scenario of a sphere undergoing translation under a prescribed force $f_p(t)$ normal to the plane. This situation is pertinent in practical applications, such as the sedimentation of a sphere under its own weight or the manipulation of particles using electric and magnetic fields [42–44]. Unlike the previous case of prescribed velocity, complexity arises in this case from the influence of viscoelasticity on the translational velocity of the sphere.

One naive approach to tackle this problem is to expand H_0 and V as regular perturbation series in Deborah number. However, this method encounters cumbersome expansions and fails to obtain

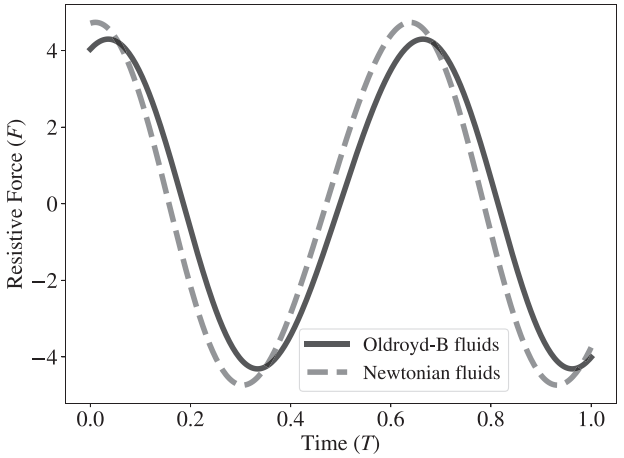

FIG. 4. The time evolution of the resistive force acting on the sphere translating towards a rigid plane with an oscillatory motion in an Oldroyd-B fluid; the sphere oscillates at a distance $h_0(0)$ from the rigid plane with an amplitude γ, described by $h_0 = h_0(0) - \gamma \sin \omega t$. Here, we set $\Gamma = \frac{\gamma}{h_0(0)} = 0.1$, $\mathrm{De} = \frac{\gamma\omega\lambda}{h_0(0)} = 0.05$, and $\beta_p = 0.5$. The dashed line represents the behavior of a Newtonian fluid, and the solid line represents the behavior of an Oldroyd-B fluid up to the second-order correction.

an asymptotically correct approximation for the long time period (we revisit this calculation in Sec. IV B). In Sec. IV A, we consider the constant force $f_p(t) = f_{\text{const}}$.

This case admits a self-consistent ansatz for the expansion of H_0 and V based on the physical intuition that the viscoelasticity will affect the sedimentation rate of the sphere when the sphere translates under a constant force. To be more precise, we observed in the previous case of a sphere translating under a prescribed velocity in Sec. III A that V/H_0 is a constant to the leading order [see (22)]. Therefore, we expect H_0 to behave like an exponential function in time. This serves as a foundation for us to posit an ansatz of the form

$$H_0(T) = \mathrm{e}^{\alpha T}, \quad \alpha = \alpha^{(0)} + \mathrm{De}\alpha^{(1)} + \cdots, \tag{34a}$$

$$V(T) = V^{(0)} + \mathrm{De}V^{(1)} + \cdots, \quad \text{where} \quad V^{(n)} = \alpha^{(n)}\mathrm{e}^{\alpha T}. \tag{34b}$$

Later in Sec. IV B, we utilize the method of multiple timescales to tackle the case of general prescribed force $f_p(t)$; this approach provides us with the same form of solution we proposed for the constant prescribed force case (34).

A. Solution for constant prescribed force

1. Leading-order solution for constant prescribed force

As demonstrated in Sec. III A, the leading-order response remains Newtonian. The radial velocity at this order retains the same form,

$$U_R^{(0)} = \frac{1}{2}\frac{\partial P^{(0)}}{\partial R} Z(Z - H). \tag{35}$$

Now, observe that the sphere's velocity contributes at every order. At the leading order, the continuity equation takes the form $\int_0^H U_R^{(0)}\,\mathrm{d}Z = -\frac{RV^{(0)}}{2}$, which results in

$$P^{(0)} = -\frac{3V^{(0)}}{2H^2}. \tag{36}$$

As previously shown, the primary contribution to the resistive force stems from the pressure along the gap, yielding

$$F^{(0)} = -2\pi \int_0^\infty \frac{3V^{(0)}R}{2H^2}\,\mathrm{d}R = -\frac{3\pi V^{(0)}}{2H_0} = -\frac{3\pi\alpha^{(0)}}{2}. \tag{37}$$

We can now equate the leading-order resistive force (37), in dimensional form using (6), with the applied constant force $f_p(t) = f_{\text{const}}$ to obtain

$$f_{\text{const}} = \left(\frac{4\mu|v(0)|a^2}{h_0(0)}\right)\left(\frac{3\pi\alpha^{(0)}}{2}\right) \quad \Longrightarrow \quad \frac{v(0)}{h_0(0)} = \frac{f_{\text{const}}}{6\pi\mu a^2}. \tag{38}$$

Equation (38) indicates that the initial velocity of the sphere is determined by both the prescribed force and the initial height of the sphere, with the sign of the initial velocity depending on the direction of the prescribed constant force acting on the sphere. In particular, we have $\alpha^{(0)} = \mathrm{sgn}(v(0)) = \mathrm{sgn}(f_{\text{const}})$.

2. First-order correction for constant prescribed force

Applying a methodology similar to our procedure for the leading-order solution, we proceed with the calculations by solving for velocity in terms of the pressure gradient using the momentum equation. Utilizing the continuity equation, we solve for the pressure, which is then integrated to determine the resistive force acting on the sphere. This method mirrors the calculations of Sec. III, with one adjustment to the continuity equation at the first-order correction, becoming $\int_0^H U_R^{(1)}\,\mathrm{d}Z = -\frac{RV^{(1)}}{2}$. For brevity, we omit these details and note that the calculations yield the formula for the first-order correction to pressure as

$$P^{(1)} = -\frac{3V^{(1)}}{2H^2} + \beta_p\left(\frac{\mathrm{d}V^{(0)}}{\mathrm{d}T}\frac{3}{2H^2} - \frac{3V^{(0)}V}{H^3} - \frac{9(V^{(0)})^2(H_0 - 4R^2)}{10H^4}\right). \tag{39}$$

Integrating (39) along the gap provides the first-order correction to the resistive force,

$$F^{(1)} = -\frac{3\pi V^{(1)}}{2H_0} + \pi\beta_p\left(\frac{\mathrm{d}V^{(0)}}{\mathrm{d}T}\frac{3}{2H_0} - \frac{3V^{(0)}V}{2H_0^2} + \frac{3(V^{(0)})^2}{10H_0^2}\right) = -\frac{3\pi\alpha^{(1)}}{2} + \frac{3\pi\beta_p(\alpha^{(0)})^2}{10}. \tag{40}$$

Given that the constant force (f_{const}) is prescribed on the sphere, it only appears at the leading order. Consequently, $F^{(1)} = 0$, which results in $\alpha^{(1)} = \frac{\beta_p}{5}$. Thus, by adopting the perturbation expansion forms for H_0 and V as in (34a) and (34b), we establish a straightforward method for determining the unknown exponents related to the height of the sphere. Notably, for the scenario in which the sphere is in its final state of sedimentation onto the wall under its own weight, we obtain

$$H_0 = \mathrm{e}^{\alpha T}, \quad \alpha = -1 + \tfrac{1}{5}\beta_p\mathrm{De} + O(\mathrm{De}^2). \tag{41}$$

We observe that the viscoelasticity influences the sedimentation rate of the sphere. Specifically, higher Deborah numbers result in a slower sedimentation process at the first order, as shown in Fig. 5.

B. Leading-order solution for general prescribed force

In this section, we provide a further examination of the analysis presented in Sec. IV A, where we relax the constraint that the forcing function $f_p(t)$ is constant; this detailed analysis serves as a foundation for the ansatz proposed in (34). First, to motivate our discussion, we seek a regular perturbation-series approach to the problem by writing

$$H_0(T) = H_0^{(0)}(T) + \mathrm{De}H_0^{(1)}(T) + \mathrm{De}^2H_0^{(2)}(T) + \cdots, \tag{42a}$$

$$V(T) = V^{(0)}(T) + \mathrm{De}V^{(1)}(T) + \mathrm{De}^2V^{(2)}(T) + \cdots, \tag{42b}$$

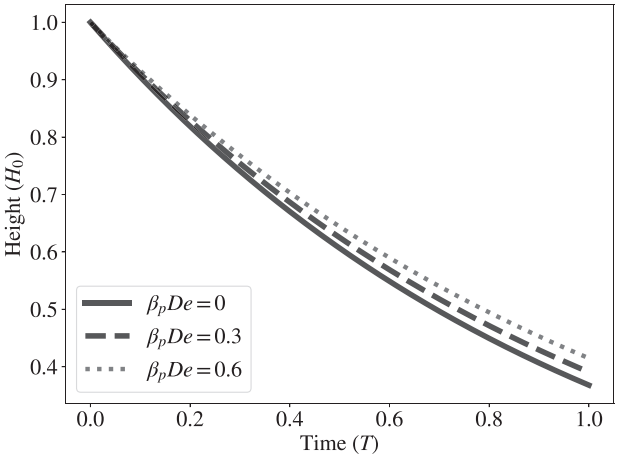

FIG. 5. The time evolution of the height of the sphere sedimenting under its own weight in an Oldroyd-B fluid, up to the first-order correction in De, for different values of β_pDe.

with $\frac{dH_0^{(n)}}{dT} = V^{(n)}$ for all n. As in Sec. IV A 1, we can proceed with the same steps to obtain

$$U_R^{(0)} = \frac{1}{2}\frac{\partial P^{(0)}}{\partial R} Z(Z-H), \quad P^{(0)} = -\frac{3V^{(0)}}{2H^2}, \quad \text{and} \quad F^{(0)} = -\frac{3\pi V^{(0)}}{2H_0}. \tag{43}$$

Note, however, that writing $F^{(0)}$ in this form is subtly misleading for comparing with the prescribed force f_p; the term H_0 in the denominator still possesses an expansion in Deborah number as suggested in (42a). Therefore, we expand

$$\frac{1}{H_0} = \frac{1}{H_0^{(0)} + \mathrm{De} H_0^{(1)} + \mathrm{De}^2 H_0^{(2)} + \cdots} \tag{44a}$$

$$= \frac{1}{H_0^{(0)}} - \mathrm{De}\left(\frac{H_0^{(1)}}{\left(H_0^{(0)}\right)^2}\right) + \mathrm{De}^2\left(-\frac{H_0^{(2)}}{\left(H_0^{(0)}\right)^2} + \frac{\left(H_0^{(1)}\right)^2}{\left(H_0^{(0)}\right)^3}\right) + O(\mathrm{De}^3), \tag{44b}$$

so that $F^{(0)}$ is given as

$$F^{(0)} = -\frac{3\pi V^{(0)}}{2H_0^{(0)}} + \mathrm{De}\left(\frac{3\pi V^{(0)} H_0^{(1)}}{2\left(H_0^{(0)}\right)^2}\right) - \mathrm{De}^2\left(\frac{3\pi V^{(0)}}{2}\right)\left(-\frac{H_0^{(2)}}{\left(H_0^{(0)}\right)^2} + \frac{\left(H_0^{(1)}\right)^2}{\left(H_0^{(0)}\right)^3}\right) + O(\mathrm{De}^3). \tag{45}$$

Using (45), we balance the leading-order term in the expansion of $F^{(0)}$ with the prescribed force f_p to obtain

$$f_p = \left(\frac{4\mu|v(0)|a^2}{h_0(0)}\right)\left(\frac{3\pi V^{(0)}}{2H_0^{(0)}}\right) \Longrightarrow \frac{v(0)}{h_0(0)} = \frac{f_p(0)}{6\pi\mu a^2}. \tag{46}$$

Now, set $F_p = \frac{f_p}{|f_p(0)|}$ so that $F_p = \frac{V^{(0)}}{H_0^{(0)}} = \frac{d}{dT}(\log H_0^{(0)})$. Integrating the latter expression with respect to time from 0 to T, we arrive at

$$H_0^{(0)} = \exp\left(\int_0^T F_p(T')\, dT'\right). \tag{47}$$

Following similar steps, we solve for the first-order correction to the velocity and pressure and find the resistive force due to the pressure distribution,

$$F^{(1)} = -\frac{3\pi V^{(1)}}{2H_0} + \pi\beta_p\left(\frac{\mathrm{d}V^{(0)}}{\mathrm{d}T}\frac{3}{2H_0} - \frac{3V^{(0)}V}{2H_0^2} + \frac{3(V^{(0)})^2}{10H_0^2}\right) \tag{48a}$$

$$= -\frac{3\pi V^{(1)}}{2H_0^{(0)}} + \pi\beta_p\left(\frac{\mathrm{d}V^{(0)}}{\mathrm{d}T}\frac{3}{2H_0^{(0)}} - \frac{3(V^{(0)})^2}{2\left(H_0^{(0)}\right)^2} + \frac{3(V^{(0)})^2}{10\left(H_0^{(0)}\right)^2}\right) + O(\mathrm{De}) \tag{48b}$$

$$= -\frac{3\pi V^{(1)}}{2H_0^{(0)}} + \pi\beta_p\left(\frac{\mathrm{d}V^{(0)}}{\mathrm{d}T}\frac{3}{2H_0^{(0)}} - \frac{6}{5}F_p^2\right) + O(\mathrm{De}). \tag{48c}$$

Combining (45) and (48), we obtain the resistive force up to the first order in De,

$$F^{(0)} + \mathrm{De}F^{(1)} = -\frac{3\pi V^{(0)}}{2H_0^{(0)}} + \mathrm{De}\left(\left(\frac{3\pi V^{(0)}H_0^{(1)}}{2\left(H_0^{(0)}\right)^2}\right) - \frac{3\pi V^{(1)}}{2H_0^{(0)}} + \pi\beta_p\left(\frac{\mathrm{d}V^{(0)}}{\mathrm{d}T}\frac{3}{2H_0^{(0)}} - \frac{6}{5}F_p^2\right)\right) + O(\mathrm{De}^2). \tag{49}$$

Given that the prescribed force, $f_p(t)$, is only present at the leading order, we set the $O(\mathrm{De})$ term to zero to obtain

$$0 = \left(\frac{3\pi V^{(0)}H_0^{(1)}}{2\left(H_0^{(0)}\right)^2}\right) - \frac{3\pi V^{(1)}}{2H_0^{(0)}} + \pi\beta_p\left(\frac{\mathrm{d}V^{(0)}}{\mathrm{d}T}\frac{3}{2H_0^{(0)}} - \frac{6}{5}F_p^2\right). \tag{50}$$

Rearranging (50), we have

$$0 = -F_pH_0^{(1)} + V^{(1)} + \beta_p\left(-\frac{\mathrm{d}V^{(0)}}{\mathrm{d}T} + \frac{4}{5}F_p^2H_0^{(0)}\right) \tag{51a}$$

$$= \frac{\partial}{\partial T}\left(\exp\left(-\int_0^T F_p(T')\mathrm{d}T'\right)H_0^{(1)}\right) - \beta_p\left(\frac{\mathrm{d}F_p}{\mathrm{d}T} + \frac{1}{5}F_P^2\right). \tag{51b}$$

Using the initial condition $H_0^{(1)}(0) = 0$, we conclude that

$$H_0^{(1)} = \beta_p\left(-\mathrm{sgn}(f_p(0)) + F_p + \frac{1}{5}\int_0^T F_p(T')^2\,\mathrm{d}T'\right)\exp\left(\int_0^T F_p(T')\,\mathrm{d}T'\right). \tag{52}$$

Thus, up to the first-order correction, we obtain

$$H_0^{(0)} + \mathrm{De}H_0^{(1)} = \left(1 + \mathrm{De}\beta_p\left(-\mathrm{sgn}(f_p(0)) + F_p + \frac{1}{5}\int_0^T F_p(T')^2\,\mathrm{d}T'\right)\right)\exp\left(\int_0^T F_p(T')\,\mathrm{d}T'\right). \tag{53}$$

For instance, when $f_p(t) = f_{\mathrm{const}}$ is a negative constant (e.g., when the sphere is sedimenting under its own weight), we have $\mathrm{sgn}(f_p(0)) = -1$ and $F_p(T) = -1$ so that (53) becomes

$$H_0^{(0)} + \mathrm{De}H_0^{(1)} = \left(1 + \tfrac{1}{5}\mathrm{De}\beta_pT\right)\mathrm{e}^{-T}. \tag{54}$$

Notice from (54) that when $T \gg \frac{1}{\mathrm{De}\beta_p}$, the first-order correction term's magnitude exceeds that of the leading-order correction term. Consequently, this asymptotic approximation loses validity for extended time periods. The emergence of an unbounded term for large T, i.e., the "secular term," motivates us to construct a solution extending beyond $T = O(\mathrm{De}^{-1})$ using the method of multiple scales. To this end, we introduce the slow timescale τ:

$$\tau = \mathrm{De}\mathcal{G}(T), \tag{55}$$

where the function $\mathcal{G}$ is yet to be determined to remove the secular terms. We posit that H_0 can be represented as a perturbation series solution dependent on both T and τ,

$$H_0(T) = H_0^{(0)}(T,\tau) + \mathrm{De} H_0^{(1)}(T,\tau) + \cdots, \tag{56}$$

so that

$$\frac{\partial H_0}{\partial T} = \underbrace{\frac{\partial H_0^{(0)}}{\partial T}}_{V^{(0)}} + \mathrm{De}\left(\underbrace{\mathcal{G}'(T)\frac{\partial H_0^{(0)}}{\partial \tau} + \frac{\partial H_0^{(1)}}{\partial T}}_{V^{(1)}}\right) + \cdots. \tag{57}$$

By comparing the prescribed force with the resistive force due to the pressure at the leading order as in (46) and (47), we have

$$H_0^{(0)} = c(\tau)\exp\left(\int_0^T F_p(T')\,\mathrm{d}T'\right), \tag{58}$$

which involves an unknown function $c(\tau)$ to be determined by matching at the next order. Using the force balance at the first-order correction (51a), we obtain

$$0 = -F_p H_0^{(1)} + V^{(1)} + \beta_p\left(-\frac{\mathrm{d}V^{(0)}}{\mathrm{d}T} + \frac{4}{5}F_p^2 H_0^{(0)}\right) \tag{59a}$$

$$= -F_p H_0^{(1)} + \mathcal{G}'(T)\frac{\partial H_0^{(0)}}{\partial \tau} + \frac{\partial H_0^{(1)}}{\partial T} + \beta_p\left(-\frac{\mathrm{d}V^{(0)}}{\mathrm{d}T} + \frac{4}{5}F_p^2 H_0^{(0)}\right) \tag{59b}$$

$$= \frac{\partial}{\partial T}\left(\exp\left(-\int_0^T F_p(T')\,\mathrm{d}T'\right)H_0^{(1)}\right) + \mathcal{G}'(T)c'(\tau) - c(\tau)\beta_p\left(\frac{\mathrm{d}F_p}{\mathrm{d}T} + \frac{1}{5}F_p^2\right). \tag{59c}$$

To remove the secular term, we set

$$\mathcal{G}'(T) = \frac{\mathrm{d}F_p}{\mathrm{d}T} + \frac{1}{5}F_p^2 \quad \text{with} \quad \mathcal{G}(0) = 0, \tag{60}$$

and

$$c'(\tau) = c(\tau)\beta_p \quad \text{with} \quad c(0) = 1. \tag{61}$$

Solving (60) and (61) results in

$$\mathcal{G}(T) = -\mathrm{sgn}(f_p(0)) + F_p(T) + \frac{1}{5}\int_0^T F_p^2(T')\,\mathrm{d}T' \quad \text{and} \quad c(\tau) = \exp(\beta_p\tau). \tag{62}$$

Thus, we obtain a leading-order approximation, valid for long times,

$$H_0^{(0)} = c(\tau)\exp\left(\int_0^T F_p(T')\,\mathrm{d}T'\right) = \exp\left(\int_0^T F_p(T')\,\mathrm{d}T' + \beta_p\tau\right) \tag{63a}$$

$$= \exp\left(\int_0^T F_p(T')\,\mathrm{d}T' + De\beta_p\left(-\mathrm{sgn}(f_p(0)) + F_p(T) + \frac{1}{5}\int_0^T F_p^2(T')\,\mathrm{d}T'\right)\right). \tag{63b}$$

For example, in the case of $F_p(t) = -1$, corresponding to the situation in which the sphere sediments due to a constant applied force, we obtain

$$H_0^{(0)} = \exp\left(\left(-1 + \tfrac{1}{5}\mathrm{De}\beta_p\right)T\right). \tag{64}$$

This serves as the foundation for the ansatz introduced in (34). In the case of a more general forcing function F_p, the complexity arising from the difference between $\int_0^T F_p(T')\,\mathrm{d}T'$ and $\int_0^T F_p^2(T')\,\mathrm{d}T'$ makes it challenging to derive a simpler form of the solution. Nevertheless, our leading-order solutions, obtained using the method of multiple scales (63), can be readily applied to scenarios involving time-varying forces, such as those generated by electric and magnetic fields.

V. CONCLUSIONS

In this work, we studied the translation of a sphere towards or away from a rigid plane in an Oldroyd-B fluid, in the low-Deborah-number limit, for two distinct situations: prescribing the sphere's translational velocity, and prescribing the force on the sphere. Employing the lubrication approximation and a perturbation expansion in powers of the Deborah number, we crafted our theoretical analysis. Our theoretical framework allowed us to obtain analytical approximations for velocity fields, pressures, and forces exerted on the sphere, and to elucidate the temporal microstructural changes as the particle-wall gap changes over time. For cases of the prescribed velocity, we obtained an analytical expression for the resistive force at the first order in De. In particular, when the sphere translates towards or away from the rigid plane with a constant velocity, we found that the viscoelasticity decreases the resistive force at $O(\mathrm{De})$ regardless of the sphere's direction, with a more pronounced effect at higher De.

Although the perturbation expansion approach can be repeatedly used to obtain the solutions for the velocity fields, pressures, and resistive forces to any order in De, this direct method involves tedious calculations at higher orders. Therefore, we leveraged the reciprocal theorem to derive higher-order corrections to the resistive force using velocity fields from preceding orders, thereby obtaining the resistive force up to the second-order correction in De. We found that, at the second order, the viscoelasticity of the polymer solution can either increase or decrease the resistive force depending on the direction in which the sphere translates near the plane. For cases in which the force is prescribed on the sphere, a more complex analysis is needed due to the influence of viscoelasticity on the sphere's translational velocity. To this end, we introduced an ansatz for a constant force scenario, and we derived solution forms for cases of prescribed forces using the method of multiple scales. Specifically, for the case in which a sphere settles under its own weight due to gravity, our study unveiled the role of viscoelasticity in shaping its descent speed. As De increases, viscoelasticity causes the sphere to settle more slowly, reducing the leading-order sedimentation rate.

Our analysis offers insights into addressing viscoelastic lubrication problems for geometries that evolve over time. In addition to a sphere translating near a plane wall, our approach can be readily extended to tackle more intricate geometries, such as those involving zero local curvature [23] or interactions between multiple spheres [15]. Since our analysis is not limited to constant velocity or force, we expect our approach to be useful to a wide range of applications, such as the design of rheological devices. While theoretical analyses of viscoelastic flows have traditionally focused on steady flows, our work provides a stepping stone for understanding how the conformation tensor changes in response to evolving geometry, shedding light on the unsteady nature of microstructures. Moreover, the use of the multiple timescale analysis, as demonstrated in Sec. IV B, introduces new tools for exploring the interplay between fluid flow and polymer relaxation in complex scenarios.

ACKNOWLEDGMENTS

E.B. acknowledges the support by Grant No. 2022688 from the U.S.-Israel Binational Science Foundation (BSF). H.A.S. acknowledges the support from Grant No. CBET-2246791 from the U.S. National Science Foundation (NSF); also, the research was partially supported by NSF through Princeton University's Materials Research Science and Engineering Center DMR-2011750.

[1] L. G. Leal, Particle motions in a viscous fluid, Annu. Rev. Fluid Mech. **12**, 435 (1980).

[2] A. Karnis and S. G. Mason, Particle motions in sheared suspensions. XIX. Viscoelastic media, Trans. Soc. Rheol. **10**, 571 (1966).

[3] A. H. Raffiee, A. M. Ardekani, and S. Dabiri, Numerical investigation of elasto-inertial particle focusing patterns in viscoelastic microfluidic devices, J. Non-Newtonian Fluid Mech. **272**, 104166 (2019).
[4] J. De Vicente, *Viscoelasticity: From Theory to Biological Applications* (IntechOpen, 2012).
[5] J. Najafi, S. Dmitrieff, and N. Minc, Size- and position-dependent cytoplasm viscoelasticity through hydrodynamic interactions with the cell surface, Proc. Natl. Acad. Sci. USA **120**, e2216839120 (2023).
[6] M. Stimson and G. B. Jeffery, The motion of two spheres in a viscous fluid, Proc. R. Soc. A **111**, 110 (1926).
[7] H. Brenner, The slow motion of a sphere through a viscous fluid towards a plane surface, Chem. Eng. Sci. **16**, 242 (1961).
[8] A. D. Maude, End effects in a falling-sphere viscometer, Br. J. Appl. Phys. **12**, 293 (1961).
[9] M. D. A. Cooley and M. E. O'Neill, On the slow motion generated in a viscous fluid by the approach of a sphere to a plane wall or stationary sphere, Mathematika **16**, 37 (1969).
[10] R. E. Hansford, On converging solid spheres in a highly viscous fluid, Mathematika **17**, 250 (1970).
[11] D. J. Jeffrey, Low-Reynolds-number flow between converging spheres, Mathematika **29**, 58 (1982).
[12] P. Brunn, Interaction of spheres in a viscoelastic fluid, Rheol. Acta **16**, 461 (1977).
[13] A. M. Ardekani, R. H. Rangel, and D. D. Joseph, Motion of a sphere normal to a wall in a second-order fluid, J. Fluid Mech. **587**, 163 (2007).
[14] A. M. Ardekani, R. H. Rangel, and D. D. Joseph, Two spheres in a free stream of a second-order fluid, Phys. Fluids **20**, 063101 (2008).
[15] R. Dandekar and A. M. Ardekani, Nearly touching spheres in a viscoelastic fluid, Phys. Fluids **33**, 083112 (2021).
[16] G. J. Rodin, Squeeze film between two spheres in a power-law fluid, J. Non-Newtonian Fluid Mech. **63**, 141 (1996).
[17] A. Vázquez-Quesada and M. Ellero, Analytical solution for the lubrication force between two spheres in a bi-viscous fluid, Phys. Fluids **28**, 073101 (2016).
[18] A. Vázquez-Quesada, N. J. Wagner, and M. Ellero, Normal lubrication force between spherical particles immersed in a shear-thickening fluid, Phys. Fluids **30**, 123102 (2018).
[19] M. J. Riddle, C. Narvaez, and R. B. Bird, Interactions between two spheres falling along their line of centers in a viscoelastic fluid, J. Non-Newtonian Fluid Mech. **2**, 23 (1977).
[20] J. G. Oldroyd, On the formulation of rheological equations of state, Proc. R. Soc. A **200**, 523 (1950).
[21] R. B. Bird, R. C. Armstrong, and O. Hassager, *Dynamics of Polymeric Liquids, volume 1: Fluid Mechanics*, 2nd ed. (Wiley, New York, 1987).
[22] A. Z. Szeri, *Fluid Film Lubrication: Theory and Design* (Cambridge University Press, Cambridge, 1998).
[23] H. A. Stone, On lubrication flows in geometries with zero local curvature, Chem. Eng. Sci. **60**, 4838 (2005).
[24] P. M. Bungay and H. Brenner, The motion of a closely-fitting sphere in a fluid-filled tube, Int. J. Multiphase Flow **1**, 25 (1973).
[25] E. Boyko and H. A. Stone, Reciprocal theorem for calculating the flow rate–pressure drop relation for complex fluids in narrow geometries, Phys. Rev. Fluids **6**, L081301 (2021).
[26] E. Boyko and H. A. Stone, Pressure-driven flow of the viscoelastic Oldroyd-B fluid in narrow non-uniform geometries: analytical results and comparison with simulations, J. Fluid Mech. **936**, A23 (2022).
[27] K. D. Housiadas and A. N. Beris, Lubrication approximation of pressure-driven viscoelastic flow in a hyperbolic channel, Phys. Fluids **35**, 123116 (2023).
[28] Y. L. Zhang, O. K. Matar, and R. V. Craster, Surfactant spreading on a thin weakly viscoelastic film, J. Non-Newtonian Fluid Mech. **105**, 53 (2002).
[29] S. Saprykin, R. J. Koopmans, and S. Kalliadasis, Free-surface thin-film flows over topography: Influence of inertia and viscoelasticity, J. Fluid Mech. **578**, 271 (2007).
[30] C. Datt, M. Kansal, and J. H. Snoeijer, A thin-film equation for a viscoelastic fluid, and its application to the Landau–Levich problem, J. Non-Newtonian Fluid Mech. **305**, 104816 (2022).
[31] J. A. Tichy, Non-Newtonian lubrication with the convected Maxwell model, Trans. ASME J. Tribol. **118**, 344 (1996).

[32] H. Ahmed and L. Biancofiore, A new approach for modeling viscoelastic thin film lubrication, J. Non-Newtonian Fluid Mech. **292**, 104524 (2021).
[33] H. Ahmed and L. Biancofiore, Modeling polymeric lubricants with non-linear stress constitutive relations, J. Non-Newtonian Fluid Mech. **321**, 105123 (2023).
[34] N. Phan-Thien, J. Dudek, D. V. Boger, and V. Tirtaatmadja, Squeeze film flow of ideal elastic liquids, J. Non-Newtonian Fluid Mech. **18**, 227 (1985).
[35] N. Phan-Thien and W. Walsh, Squeeze-film flow of an Oldroyd-B fluid: Similarity solution and limiting Weissenberg number, Z. Angew. Math. Phys. **35**, 747 (1984).
[36] N. Phan-thien, F. Sugeng, and R. I. Tanner, The squeeze-film flow of a viscoelastic fluid, J. Non-Newtonian Fluid Mech. **24**, 97 (1987).
[37] N. Phan-Thien and H. T. Low, Squeeze-film flow of a viscoelastic fluid a lubrication model, J. Non-Newtonian Fluid Mech. **28**, 129 (1988).
[38] O. Reynolds, On the theory of lubrication and its application to Mr. Beauchamp Tower's experiments, including an experimental determination of the viscosity of olive oil, Philos. Trans. R. Soc. London **177**, 157 (1886).
[39] J. Happel and H. Brenner, *Low Reynolds Number Hydrodynamics*, 2nd ed. (Martinus Nijhoff, The Hague, 1983).
[40] L. Jawerth, E. Fischer-Friedrich, S. Saha, J. Wang, T. Franzmann, X. Zhang, J. Sachweh, M. Ruer, M. Ijavi, S. Saha, J. Mahamid, A. A. Hyman, and F. Jülicher, Protein condensates as aging Maxwell fluids, Science **370**, 1317 (2020).
[41] X. Li, J. van der Gucht, P. Erni, and R. de Vries, Active microrheology of protein condensates using colloidal probe-AFM, J. Colloid Interface Sci. **632**, 357 (2023).
[42] R. T. Bonnecaze and J. F. Brady, A method for determining the effective conductivity of dispersions of particles, Proc. R. Soc. London A **430**, 285 (1990).
[43] H. V. Ly, F. Reitich, M. R. Jolly, H. T. Banks, and K. Ito, Simulations of particle dynamics in magnetorheological fluids, J. Comput. Phys. **155**, 160 (1999).
[44] S. S. Tsai, J. S. Wexler, J. Wan, and H. A. Stone, Microfluidic ultralow interfacial tensiometry with magnetic particles, Lab Chip **13**, 119 (2013).